EARTHQUAKE ENGINEERING AND STRUCTURAL DYNAMICS
Earthquake Engng. Struct. Dyn. **28**, 921–940 (1999)

SAMPLED-DATA H_2 OPTIMAL OUTPUT FEEDBACK CONTROL FOR CIVIL STRUCTURES

SESHASAYEE ANKIREDDI[†] AND HENRY T. Y. YANG*[,‡]
Department of Mechanical and Environmental Engineering, University of California, Santa Barbara, CA 93106, USA

SUMMARY

An optimal control method involving sampled data is considered for use in earthquake and wind engineering applications. The structure is modelled as a continuous system attached to a discrete-time controller using zero-order sample-and-hold devices. Examples of two buildings with active base isolators and a 163 m tall planar frame with an active mass damper are considered. The buildings with the base isolators are subjected to excitation input using the 1940 El Centro earthquake (NS component) as an example, while the planar frame is subjected to assumed sinusoidal gusts with a period close to that of the frame. The controlled responses (with and without time delays) are studied. To further analyze the features of the control designs, the building examples with base isolators are subjected to five other different earthquake excitation records. Trends in control performance and effectiveness are presented and discussed. The results suggest that such systems are potentially suited for implementation in the vibration control of civil infrastructures; such potentiality becomes more realistic with the current trends in software development and the increased use of digital computers. Copyright © 1999 John Wiley & Sons, Ltd.

KEY WORDS: sampled data, structural control, civil, earthquake, wind, mass dampers, base isolators

1. INTRODUCTION

In the last two to three decades, the use of control technology to reduce potential damage caused to civil infrastructural facilities due to earthquakes and strong winds has become an area of interest to researchers and practicing engineers.

Much effort has been devoted to the development of control devices and algorithms. Base isolators, tuned mass dampers, liquid sloshing dampers, and active tendons are examples of some devices that have been proposed and studied, and some progress has been made in implementations, either in laboratory-scale studies[1,2] or in actual applications.[3] Numerous algorithms, either indigenously developed or borrowed from the mathematical theory of control have been studied for potential use in civil structural control.

* Correspondence to: Henry T. Y. Yang, Department of Mechanical and Environmental Engineering, University of California, Santa Barbara, CA 93106, U.S.A.
† Postdoctoral Researcher
‡ Professor of Mechanical and Environmental Engineering and Chancellor, and Member ASCE
Contract/grant sponsor: National Science Foundation; Contract/grant number: 9496273-CMS

CCC 0098–8847/99/090921–20$17·50

Received 10 May 1998
Revised 23 February 1999

The increasing use of digital computers has made the development of software and implementation of digital controllers more realistic. Such controllers have several preferable features as compared to conventional analog controllers, although they do have their own set of disadvantages.[4] Both digital and analog control systems are comparable in terms of initial set-up costs. In the long run, however, it is expected that the digital controllers are relatively simpler to tune and easier to maintain than the analog controllers, and end up being more cost effective.

In this study, a sampled data control system is investigated for structural applications. It consists of a digital controller which is connected to the structure via A/D and D/A converters and sample/hold circuits. The response of the structure is sampled every ΔT seconds (the sampling interval) and a control signal is generated, which is then applied to the structure using a zero-order hold device. An optimal control technique developed by Khargonekar and Sivashankar[5] is used here. To illustrate the applicability and features of the controller, examples of two buildings with linear active base isolators and an example of a 163 m tall planar frame with a rooftop active mass damper are considered. The buildings with the base isolators are assumed to be subjected to the NS component of the 1940 El Centro earthquake, while the planar frame is subjected to simple sinusoidal gusts whose period is close to the fundamental period of the frame. The controlled responses are examined, both with and without time delay. To further examine the control designs, the building examples with base isolators are subjected to five other different seismic excitation records. Results on the performance and effectiveness are presented and discussed, with concluding remarks on the potential of such control systems in future studies, development, and implementations.

2. FORMULATION

Let the dynamic motion of the civil structure be described by

$$[M]\{\ddot{q}\} + [D]\{\dot{q}\} + [K]\{q\} = [F_0]w + [B_0]u \tag{1}$$

Here $[M]$, $[D]$ and $[K]$ are the $(n_0 \times n_0)$ inertia, damping and stiffness matrices of the system, $\{q\} \in R^{n_0}$ is the displacement vector, $u \in R^{m_2}$ is the vector of control forces, $[F_0]w$ is the external disturbance, and $[B_0] \in R^{n_0 \times m_2}$ describes the control force locations.

Let $z \in R^{p_1}$ represent a vector of controlled outputs for the structure. Thus, for instance, the roof displacement/acceleration or the interstory drifts may be elements of z. It is also assumed that certain noise-free measured outputs, which are represented by the vector y, are available for feedback. The standard state-space description of the above system is

$$\dot{x} = Ax + B_1 w + B_2 u, \quad z = C_1 x + D_{12} u, \quad y = C_2 x \tag{2}$$

In Figure 1(a), the above described 'plant' is represented as the block G. The structure is connected to a discrete time controller, represented by the block K. The measured data y passes through the block S_T which 'reads' the sensor data every ΔT seconds and treats the measurements as being constant between successive sampling instants.

The sampled information is assumed to be corrupted by a discrete-time white gaussian noise process $v(k)$ and is used by the controller K to produce a discrete-time control signal ψ, which is channelled through a zero-order hold operator, H_T, with the same time period ΔT. The input to

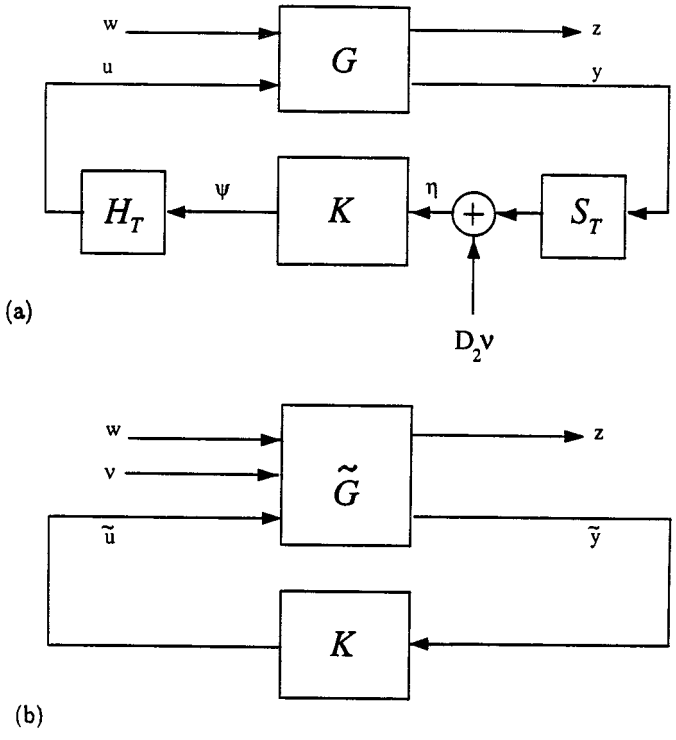

Figure 1. (a) Block diagram of the original sampled data system; (b) the H_2 equivalent discrete system

the controller block (η) and the control signal (u) are described by

$$\eta(k) = C_2 x(k\,\Delta T) + D_2 v(k), \quad u(t) = \psi(k),\ k\,\Delta T < t \leqslant (k+1)\Delta T \tag{3}$$

It is noted that u changes only every ΔT seconds, and that in between any two succesive sampling times it is constant. This is a feature of the zero-order hold operator H_T.

Thus the controller is seen to be a discrete system connected to the continuous plant G in such a way that (i) sensor data is sampled only every ΔT seconds (with measurements assumed constant between successive sampling instants), and (ii) a control signal u, which only changes every ΔT seconds (and is assumed constant during those ΔT seconds) is generated and applied to the structure. In this study, an H_2 optimal control method developed by Khargonekar and Sivashankar[5] is used for designing the controller K, which has the structure

$$\xi(k+1) = \Phi\xi(k) + \Gamma\eta(k), \quad \psi(k) = \Theta\xi(k) + \Upsilon\eta(k) \tag{4}$$

For exponentially stable linear continuous-time periodic systems, the H_2 norm of the transfer function $h(t,\tau)$ from an exogenous disturbance $w(\cdot)$ to the output z is

$$\|\mathscr{F}\|_2 \triangleq \left[\frac{1}{T}\int_0^T \left\{\int_\tau^\infty \operatorname{trace}(h(t,\tau)h^T(t,\tau))\,\mathrm{d}t\right\}\mathrm{d}\tau\right]^{1/2} \tag{5}$$

For the present sampled-data system the above definition needs to be modified[5] to account for the noise term v. The input–output map and $\|\cdot\|_2$ norm for this hybrid system are

$$z(t) = \int_0^t h_w(t,\tau)w(\tau)\,\mathrm{d}\tau + \sum_{i=0}^{k} h_v(t - i\Delta T)v(i) \tag{6}$$

$$\|\mathscr{F}\|_2 \triangleq \left[\frac{1}{T}\int_0^T \left\{\int_\tau^\infty \mathrm{trace}(h_w(t,\tau)h_w^T(t,\tau))\,\mathrm{d}t\right\}\mathrm{d}\tau + \int_0^\infty \mathrm{trace}(h_v(t)h_v^T(t))\,\mathrm{d}t\right]^{1/2} \tag{7}$$

Let it be supposed that the triplet (A, B_2, C_2) is stabilizable and detectable, and that ΔT always lies outside a set $\mathscr{T}$ (the set of all intervals ΔT_i such that either $(\mathrm{e}^{A\Delta T_i}, \int_0^{\Delta T_i}\mathrm{e}^{A\tau}B_2\,\mathrm{d}\tau)$ is not stabilizable or $(C_2, \mathrm{e}^{A\Delta T_i})$ is not detectable in discrete time). Then the H_2 norm of the present hybrid sampled data system, as defined, is exactly equal to the standard H_2 norm of an equivalent linear discrete-time system with a discrete-time controller (Figure 1(b)).[5] Also, if there exists a discrete controller system which internally stabilizes the equivalent discrete system $\tilde{G}$ and minimizes the standard transfer function H_2 norm, then the same controller minimizes the H_2 norm (equation (7)) of the corresponding sampled data system (Figure 1(a)).

Thus the process of constructing an H_2-norm optimal controller for the hybrid sampled data system consists of first determining the 'equivalent' discrete-time system $\tilde{G}$ and calculating the controller parameters $(\Phi, \Gamma, \Theta, \Upsilon)$ that minimize the standard H_2 norm of the discrete system transfer function. The construction of the discrete-time controller for the discrete equivalent system is a classical problem in optimal control and is not detailed here.

3. NUMERICAL RESULTS

To illustrate the performance of the controller, examples of a five-storey building and an eight-storey building (each with a linear active base isolator) and an example of a 163 m planar frame (with a rooftop active mass damper) were considered. The five- and eight-storey buildings were assumed to be subjected to the NS component of the 1940 El Centro earthquake, while the planar frame was subjected to sinusoidal wind gusts whose period was assumed to be close to the natural time period of the frame.

The five-storey building example (Figure 2(a)) was studied by Kelley *et al.*[6] to demonstrate Lyapunov-based active base isolator design. The floor masses were assumed to be identically equal to $m_i = 5897$ kg. The inter-storey stiffnesses were assumed as $k_i = 33\,732$, 29 093, 28 621, 24 954; and 19 059 kN/m for floors $i = 1, \ldots, 5$, respectively, while the inter-storey damping coefficients were as assumed as $c_i = 67$, 58, 57, 50 and 38 kN s/m for floors $i = 1, \ldots, 5$, respectively. The base had a mass of $m_\mathrm{b} = 6800$ kg, and its stiffness and damping coefficients were assumed to be given by $k_\mathrm{b} = 1200$ kN/m and $c_\mathrm{b} = 2{\cdot}4$ kN s/m. To validate the model, the response of the passively isolated building (to the seismic excitation) was simulated using the Newmark-β method with a time step of 0·01 s and simulation parameters $\alpha = 0{\cdot}25$, $\beta = 0{\cdot}50$, and was matched with the results presented by Kelley *et al.*[6] The simulation revealed that the building had a time period $T = 1$ s approximately.

The eight-storey building (Figure 2(b)), modelled as a set of shear beams has been studied by Yang *et al.*[7] It was assumed that the masses of all the floors were identical and equal to $m_i = 345{\cdot}6$ metric tons. The stiffnesses of the floor levels were assumed as $k_i = 340\,000$, 326 000, 285 000, 269 000, 243 000, 207 000, 16 900 and 137 000 kN/m, for floors $i = 1, \ldots, 8$, respectively; and the

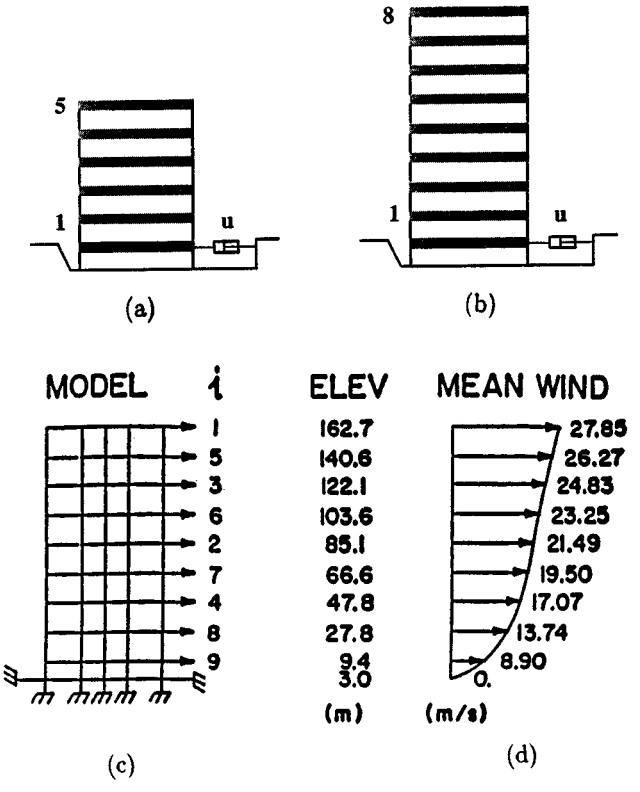

Figure 2. The earthquake engineering examples: (a) The five storey shear beam, (b) the eight storey shear beam[7] and the wind engineering example: the planar frame,[8] (c) schematic view; (d) mean wind speed distribution

damping coefficients were assumed as $c_i = 490$, 467, 410, 386, 348, 298, 243, and 196 kN s/m for $i = 1, \ldots, 8$, respectively. The mass of the base, m_b, was assumed to be 450 metric tons; its viscous damping coefficient, c_b, was assumed to be 26·17 kN s/m; and the stiffness of the base isolation system was assumed to be 18 050 kN/m. The uncontrolled building had a natural frequency 5·24 rad/s for the first mode with damping ratio 0·38 per cent. With passive base isolation, the natural frequency of the first mode was 2·2 rad/s with damping ratio of 1·6 per cent.

The planar frame building example (Figure 2(c)), from the study by Saul *et al.*,[8] had a height of 162·7 m and was simplified to have only nine translational degrees of freedom. The natural frequencies of this nine DOF model were 0·177, 0·491, 0·766, 1·032, 1·325, 1·609, 1·890, 2·163 and 3·547 Hz. The structure was assumed to be Rayleigh damped, with damping ratios 1·5 and 0·75 per cent for the first two modes, respectively. Figure 2(c) shows the Planar Frame Model with the mean wind velocity distribution along the height. The mass, stiffness and damping matrices for the structure were assumed to be those prescribed by Saul *et al.*[8] In this study, this building was assumed to have a 1 per cent mass ratio passive tuned mass damper. The damper mass was assumed to be $2{\cdot}271 \times 10^4$ kg; its stiffness was assumed to be $2{\cdot}761 \times 10^4$ N/m; and its damping constant was assumed to be $2{\cdot}492 \times 10^3$ N s/m. The passive damper properties were based on the

design formulae by Kareem.[9] For the wind disturbance, the turbulence intensities at heights of 9·4, 66·6 and 122·1 m were determined[10] to be 0·4883, 0·2231, and 0·1751, respectively. For simplicity it was assumed that the turbulence intensities were 0·4883 (up to a height of 47·8 m), 0·2231 (for a height between 47·8 and 103·6 m), and 0·1751 (for a height greater than 103·6 m). Sinusoidal wind gusts with a period of 5·5 s and with amplitudes equal to 25 per cent of the r.m.s. gust velocity at any floor were used for the planar frame.

For the five- and eight-storey examples, displacements of the base floor and the roof were assumed to be available for feedback. For the planar frame, only displacements of the roof and the mass damper were used for the feedback. For all examples studied, the objective was to minimize the roof displacement response, while simultaneously exercising some constraint on the amount of control energy. For this purpose, the two elements of the vector z (namely roof displacement and control force) were weighted by scalars α and β, respectively, to study the effects of adjusting the weights. If $\alpha \gg \beta$, then the objective function would tend to reduce the roof displacement with very little penalty on the available control resources (and vice versa). This would result in good control performance at the expense of large control forces. Without loss of generality, the scalar weight β was set to 1, since the relative ratio of the scalars is important and not their absolute values. Physically, α directly influences the 'size' of the controller gains: the larger the value of α, the larger the gains will be.

By the Nyquist Sampling Theorem,[4] to reconstruct the structural response, the measured variables need to be sampled at a frequency at least twice the dominant structural frequency. In other words, the largest sampling interval for the example buildings is at most one-half of the natural period of the buildings. Accordingly, a series of simulations were carried out for the example buildings (with a simulation time of 20 s for the five- and eight- storey buildings and 30 s for the planar frame) with different sampling intervals. In each case, the passively and actively controlled responses were evaluated by computing physical measures such as the RMS roof displacements and the control force. Three performance measures were defined: (i) S_0, the ratio of the actively- and passively- controlled roof displacement standard deviations during the simulation, (ii) P_0, the ratio of the peak actively- and passively- controlled responses, and (iii) σ_u/W, the ratio of the control force standard deviation to the weight of the structure. The results of the numerical studies are presented in Figures 3–14.

For the five-storey shear beam example (period $T = 1{\cdot}12$ s), the sampling intervals considered were $\Delta T = 0{\cdot}01$, 0·10, 0·20, 0·30 and 0·40 s, giving the sampling ratios $\Delta T/T = 0{\cdot}89$, 8·90, 17·86, 26·79 and 35·71 per cent, respectively. For the eight-storey shear beam (period $T = 2{\cdot}85$ s), the sampling intervals were $\Delta T = 0{\cdot}01$, 0·25, 0·50, 0·75 and 1·00 s, giving the sampling ratios $\Delta T/T = 0{\cdot}35$, 8·77, 17·54, 26·32 and 35·09 per cent, respectively. For the planar frame (period $T = 5{\cdot}66$ s) the chosen sampling intervals were $\Delta T = 0{\cdot}01$, 0·50, 1·00, 1·50 and 2·00 s, giving the sampling ratios $\Delta T/T = 0{\cdot}18$, 8·83, 17·67, 26·50 and 35·34 per cent, respectively. Thus for each example, the largest sampling interval studied was less than one-half the fundamental period.

Figures 3(a) and 3(b) show the variation of S_0 and P_0 with the parameter α (for different sampling intervals) for the five-storey shear beam model. When $\alpha = 0$, both S_0 and P_0 are equal to one, indicating that the active controller is no different from the passive controller. For any given $\Delta T/T$, as the value of α increases, the control performance improves as shown by the decreasing values of S_0 and P_0. However, it was noted that α may not be increased indefinitely, and that beyond a certain value (which varies depending on the sampling ratio $\Delta T/T$) there is an onset of numerical instability. The curves shown in Figure 3 (and also in subsequent figures) correspond to 'numerically stable' simulations.

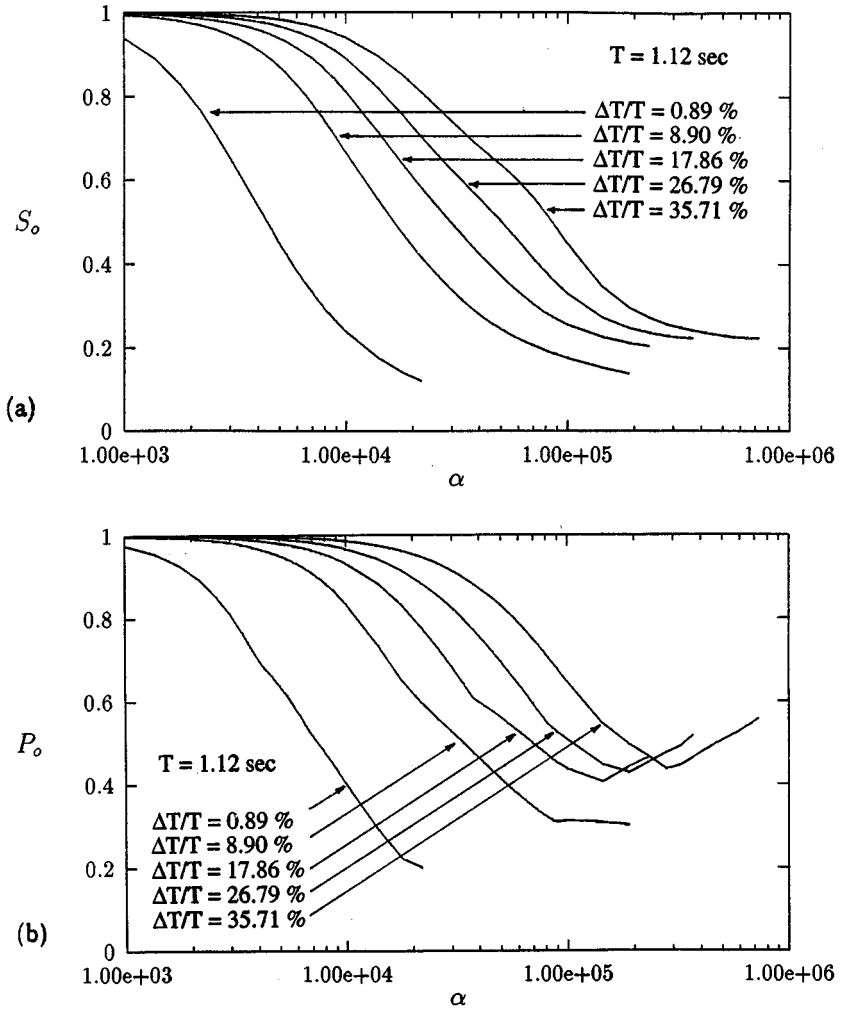

Figure 3. Control performance for the five storey shear beam model with an active base isolator for different sampling intervals. S_0 is the ratio of roof displacement standard deviations (active isolation/passive isolation), P_0 is the ratio of peak roof displacements (active isolation/passive isolation) and α is the scalar weight in the performance objective

It is noted from Figure 3(a) that the roof displacement standard deviation ratio S_0 may be reduced to less than 50 per cent for all sampling intervals considered. Similar trends are seen in the peak ratio P_0 also; although these are only typical of the current example and may not be generalized. Intuitively, although it appears that best control performance should correspond to almost continuous sampling (i.e. $\Delta T/T = 0{\cdot}89$ per cent in this case), Figure 3 shows that this need not be the case, for even with the largest sampling interval considered ($\Delta T/T = 35{\cdot}71$ per cent) the same level of control performance may be achieved by suitably large value of α.

Figures 4 and 5 show similar results obtained for the remaining building examples. The trends of the curves in these figures are generally the same as in Figure 3, although quantitatively the

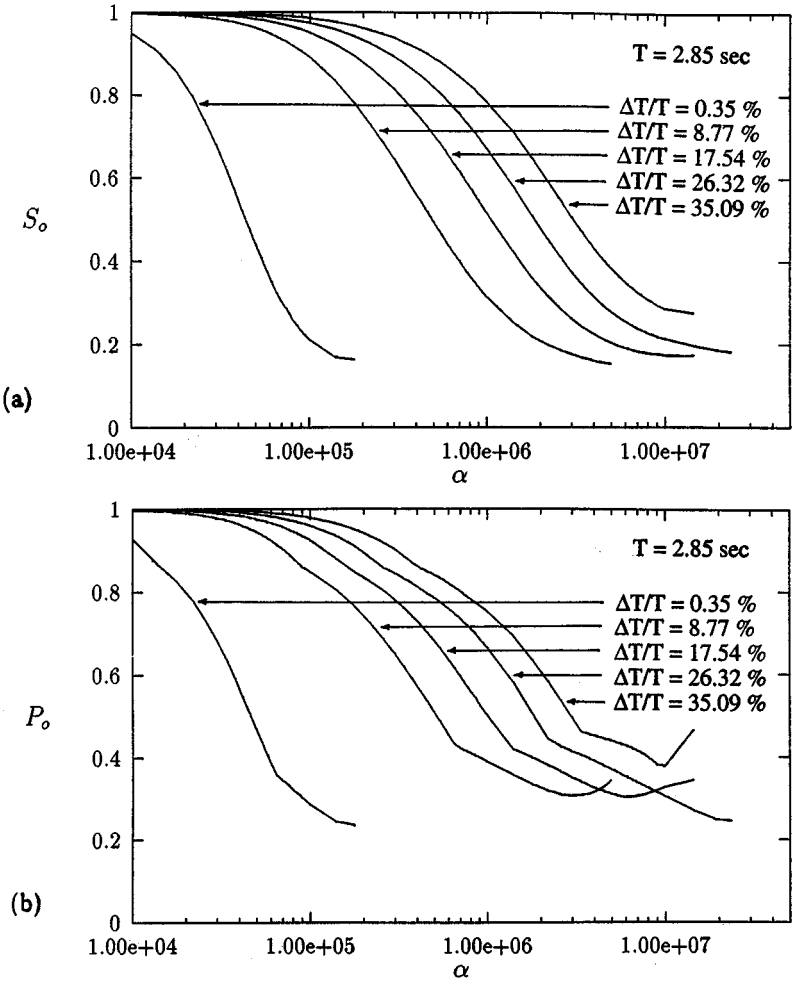

Figure 4. Control performance for the eight storey shear beam model with an active base isolator for different sampling intervals. S_0 is the ratio of roof displacement standard deviations (active isolation/passive isolation), P_0 is the ratio of peak roof displacements (active isolation/passive isolation) and α is the scalar weight in the performance objective

values of (S_0, P_0) and α are different. For the eight storey shear beam example (Figure 4), the sampled data controller can reduce the roof displacement standard deviation ratio S_0 by at least 50 per cent for all sampling intervals considered, while these reductions are less for the planar frame under wind excitation (Figure 5). It is noteworthy that for the five- and eight- storey shear beam examples, the curves for S_0 decrease uniformly and show a tendency to flatten near the value $S_0 = 0{\cdot}20$–$0{\cdot}30$, while those for the planar frame decrease uniformly but do not exhibit any flattening trend. In fact, in the case of the planar frame, for the largest sampling interval considered, $\Delta T = 2$ s ($\Delta T/T = 35{\cdot}34$ per cent), the control performance can be at best 12 per cent better than the passive mass damper. This seems to suggest that for certain building applications,

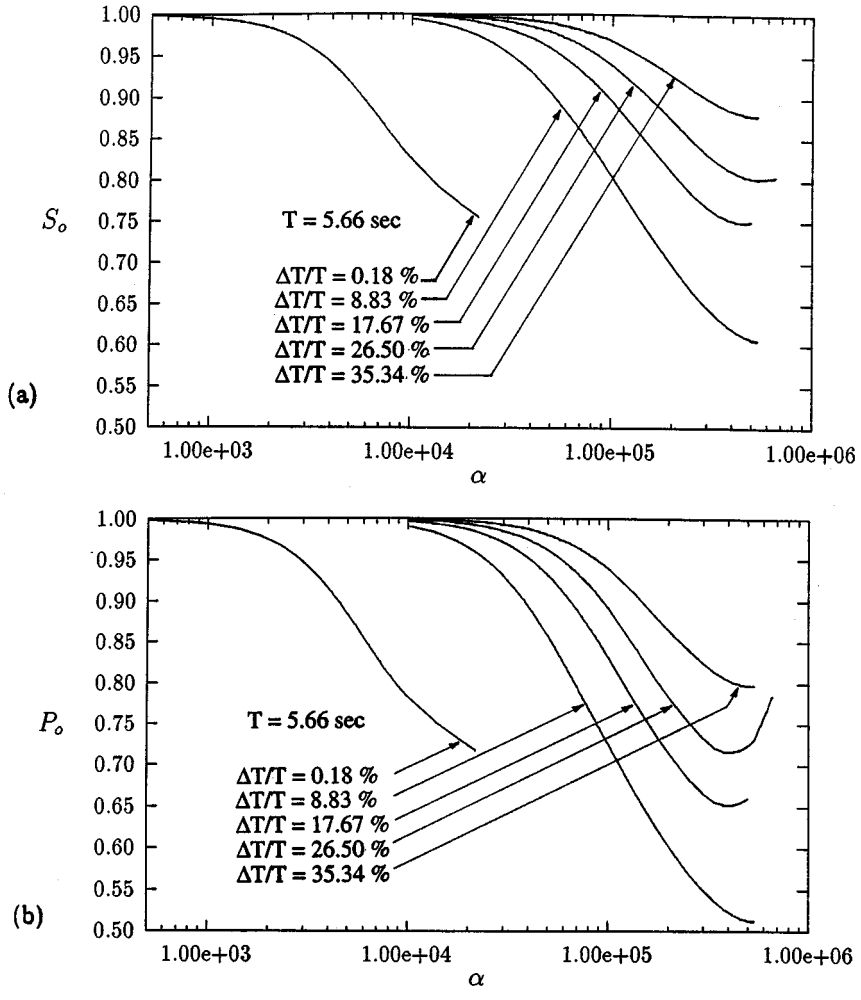

Figure 5. Control performance for the planar frame with a rooftop active mass damper for different sampling intervals. S_0 is the ratio of roof displacement standard deviations (active damper/passive damper), P_0 is the ratio of peak roof displacements (active damper/passive damper) and α is the scalar weight in the performance objective

choosing too large a sampling interval (even if it were close to but less than one-half of the natural period of the building) may have less effect on the control performance.

Figures 6–8 illustrate the trade-off behaviour of control effectiveness versus the control resources. In these figures, the ratio of RMS roof displacements, S_0, is plotted against the ratio of control force standard deviation to the weight of the structure. When the active controller is absent, $\sigma_u = 0$, and then $S_0 = 1$, hence each of the curves has a left-hand asymptotic value of '1', although this is not shown in the figures. It is not unexpected that with a few exceptions, for any given level of control effectiveness which can be achieved (i.e. for any fixed value of S_0), most frequent sampling (i.e. almost continuous sampling with $\Delta T = 0.01$ s) requires the least control

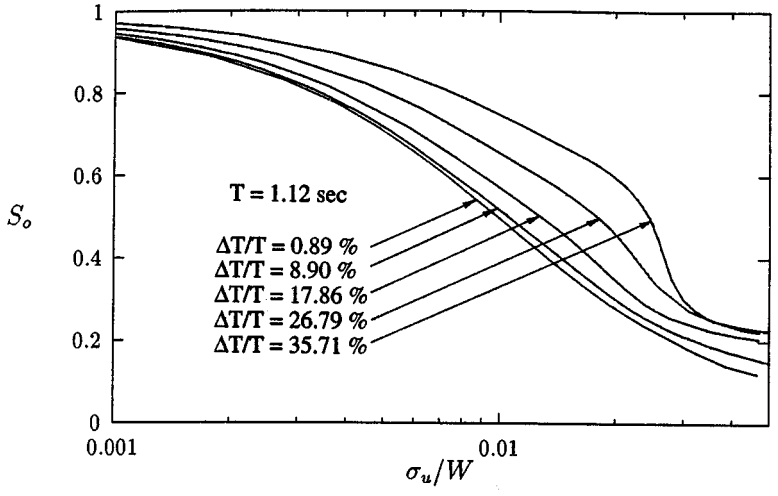

Figure 6. Trade-off curves for the five storey shear beam model with an active base isolator for different sampling intervals. S_0 is the ratio of roof displacement standard deviations (active isolation/passive isolation) and σ_u/W is the ratio: (control force standard deviation/weight of the building)

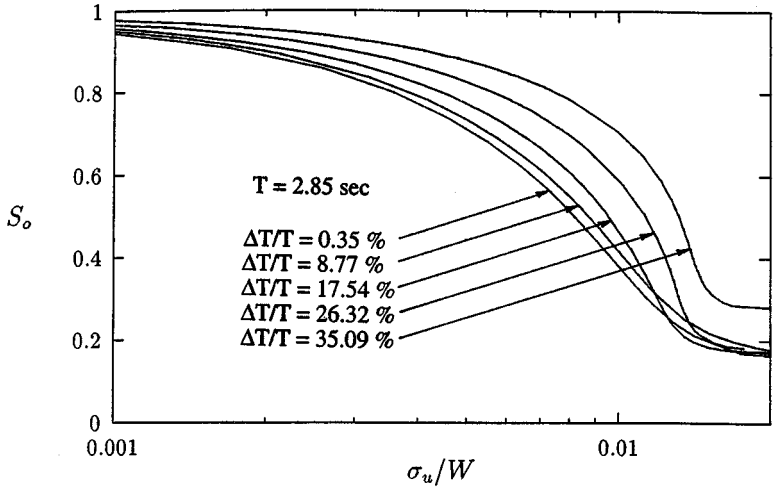

Figure 7. Trade-off curves for the eight storey shear beam model with an active base isolator for different sampling intervals. S_0 is the ratio of roof displacement standard deviations (active isolation/passive isolation) and σ_u/W is the ratio: (control force standard deviation/weight of the building)

energy, while the least frequent sampling requires the most. In other words, it is still possible to achieve the same level of control effectiveness by sampling the structural response less frequently, although the price to be paid is an increase in the amount of control energy required. The curves in Figures 6–8 show intuitive trends, namely they all start at the asymptotic value of '1' and

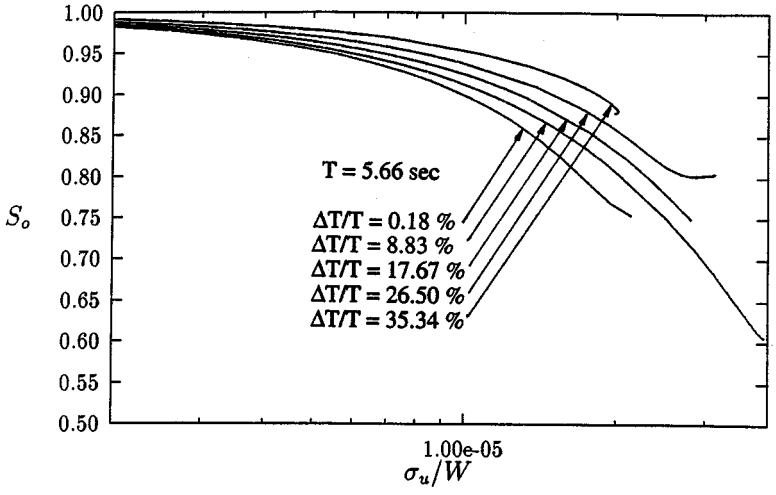

Figure 8. Trade-off curves for the planar frame with a rooftop active mass damper for different sampling intervals. S_0 is the ratio of roof displacement standard deviations (active damper/passive damper) and σ_u/W is the ratio: (control force standard deviation/weight of the building)

decrease as the control force increases. As noted before, the curves for the five- and eight- storey shear beam examples tend to decrease and flatten; such a flattening trend is not observed for the planar frame (Figure 8). Further, although control performance curves are relatively less pronounced in the planar frame (wind engineering application) as compared to the other (seismic engineering) examples, the amounts of control energy required are also much smaller.

Figures 9–11 show response time histories of the example buildings with passive and active control, for one selected combination of the weight α and the sampling interval ΔT. These are: (i) for the five-storey building, $\alpha = 1{\cdot}45 \times 10^5$ and $\Delta T/T = 35{\cdot}71$ per cent, which resulted in $S_0 = 0{\cdot}35$ and $P_0 = 0{\cdot}54$; (ii) for the eight-storey building, $\alpha = 5{\cdot}80 \times 10^6$ and $\Delta T/T = 35{\cdot}09$ per cent, which resulted in $S_0 = 0{\cdot}36$ and $P_0 = 0{\cdot}43$; (iii) for the planar frame, $\alpha = 5{\cdot}0 \times 10^5$ and $\Delta T/T = 35{\cdot}34$ per cent, which resulted in $S_0 = 0{\cdot}75$ and $P_0 = 0{\cdot}66$. Thus in Figures 9(a), 10(a) and 11(a), the dotted line is for the passively controlled system, while the solid line corresponds to the current sampled data active control. The time history of the control forces are shown in Figures 9(b), 10(b) and 11(b), respectively. As expected, the control force is constant between any two successive sampling instants.

In this study, for simplicity, the actuator dynamics were not included. The applicability of the current method would depend on the ability of the actuators to actually follow (i.e. track) the required control signal. For this, the actuator dynamics should be such that transients introduced at the sampling instant (i.e. when the control signal changes) are damped out quickly. If the time required to damp out actuator transients is much smaller than the sampling interval, then the physically applied control force would be 'similar' to that shown in Figures 9(b), 10(b) and 11(b), and the control performance would be good. If this were not the case, then the actuator may have the effect of worsening (as opposed to improving) the control performance.

However, if the sampling interval were large (while still being less than one-half the dominant period of the structure), the requirement that the actuator transients be damped quickly may be

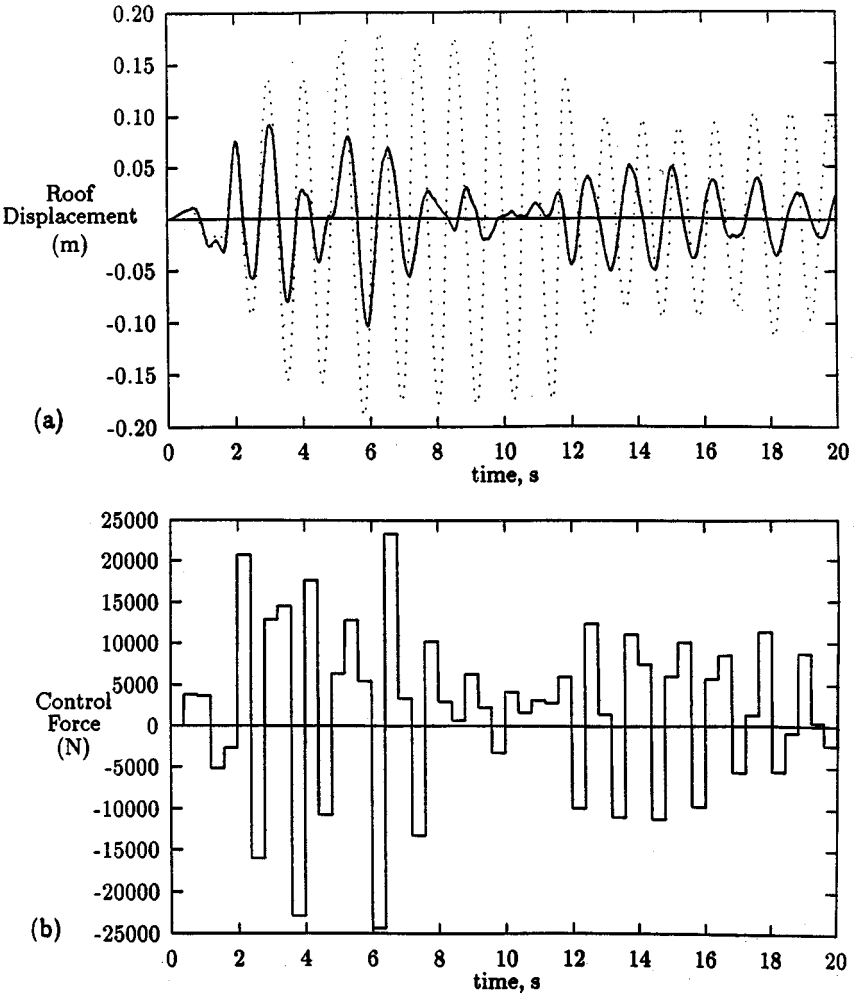

Figure 9. A sample simulation for the five storey shear beam model, with $\Delta T = 0{\cdot}4$ s: (a) the time history of the roof displacement with passive and active base isolation; (b) the time history of the control force. For this simulation, $\alpha = 1{\cdot}45 \times 10^5$, and this resulted in $S_0 = 0{\cdot}35$, $P_0 = 0{\cdot}54$

somewhat relaxed, and good control performance may still be obtained. Since large sampling intervals may be employed only for structures with relatively longer time periods, it appears that sampled data control systems may be more suited for civil structures which have relatively low natural frequencies compared to those of say, mechanical systems.

The H_2 control technique[5] used here assumes that no time delays are involved in the application of the control force. In an attempt to make the current study more realistic, a series of numerical simulations were conducted, assuming a finite (known) time delay between the computation of the control force and its actual application. The same controllers that were used for the discussions in Figures 3–11 were used when studying the effects of time delay.

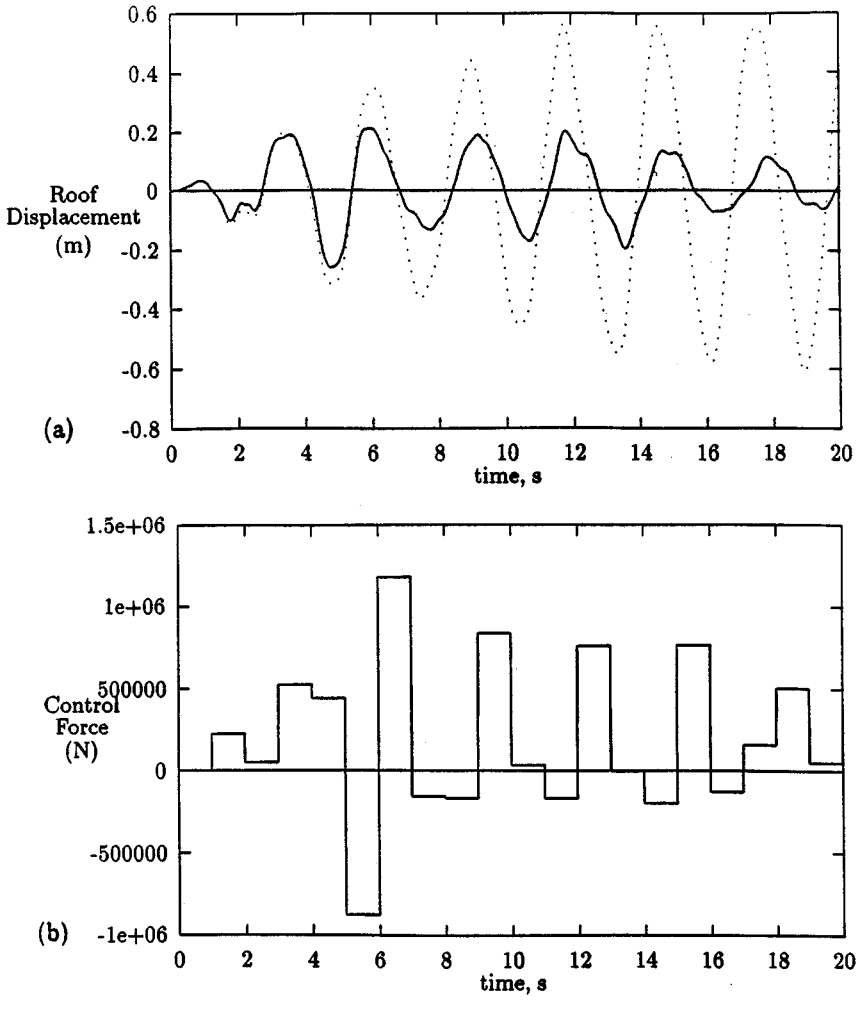

Figure 10. A sample simulation for the eight storey shear beam model, with $\Delta T = 1{\cdot}0$ s: (a) the time history of the roof displacement with passive and active base isolation; (b) the time history of the control force. For this simulation, $\alpha = 5{\cdot}80 \times 10^6$, and this resulted in $S_0 = 0{\cdot}36$, $P_0 = 0{\cdot}43$

In the case of the five-storey shear beam example, the sampling interval $\Delta T = 0{\cdot}4$ s was selected and the effects of five time delays (δ) ranging between 0 and 100 per cent of the sampling interval were simulated; these results are presented in Figures 12(a) and 12(b). Similarly, a sampling interval of $\Delta T = 1$ s was assumed for the eight-storey shear beam and the planar frame, and the results for these examples are presented in Figures 13 and 14, respectively.

Figure 12 shows that if the time delay ratio $\delta/\Delta T$ is less than 75 per cent, the performance of the controller is largely unaffected. However if the delay is of the order of the sampling interval ($\delta/\Delta T = 100$ per cent) the control performance is visibly affected, as may be seen from

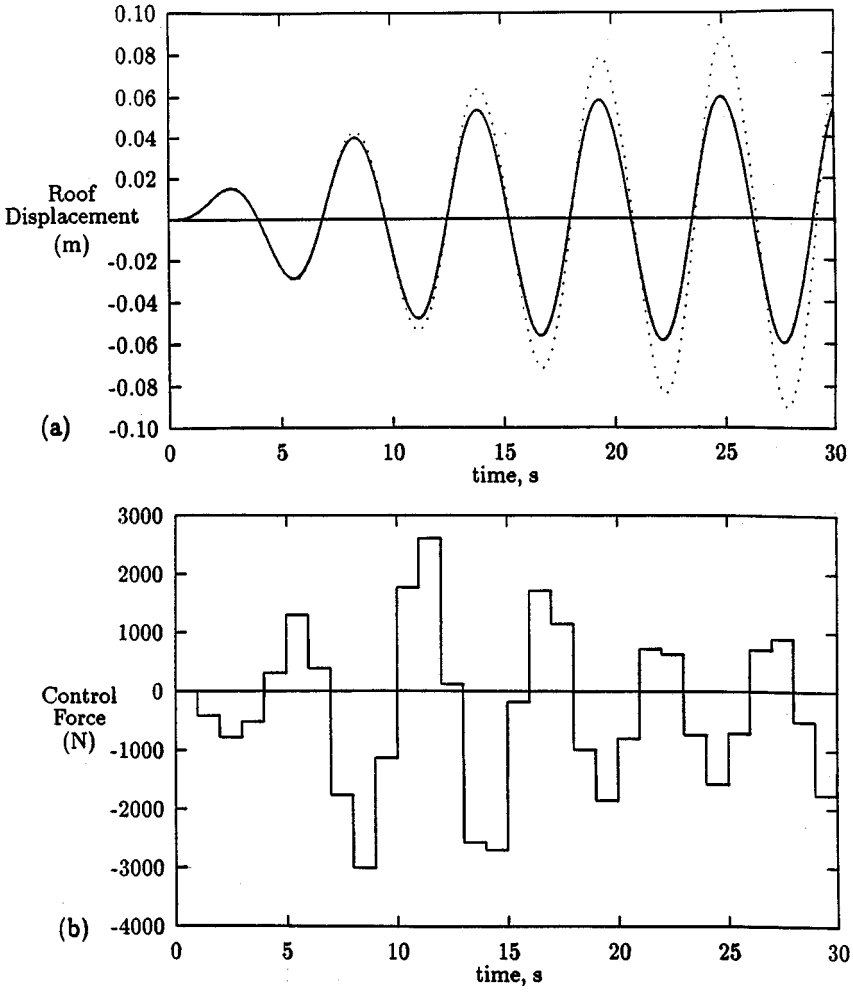

Figure 11. A sample simulation for the planar frame, with $\Delta T = 1{\cdot}0$ s: (a) the time history of the roof displacement with rooftop passive/active mass dampers; (b) the time history of the control force. For this simulation, $\alpha = 5{\cdot}00 \times 10^5$, and this resulted in $S_0 = 0{\cdot}75$, $P_0 = 0{\cdot}66$

Figures 12(a) and 12(b). The intertwining behaviour of the curves in Figure 12(a), for large values of α, may be due to possible numerical inaccuracies; thus for instance it may not be inferred that for some ranges of α, small amounts of time delay may slightly improve the control performance (as compared to the case with no time delay). These observations regarding the effects of time delay are for the specific five-storey shear beam example and the sampling interval considered, and may not be treated as being representative of the general case.

Figure 13 reveals that the effects of time delay for the eight-storey shear beam model are similar (in trend) to those for the five-storey shear beam model. When the time delay δ is of the order of the sampling interval the control performance is markedly poorer as compared to the case with

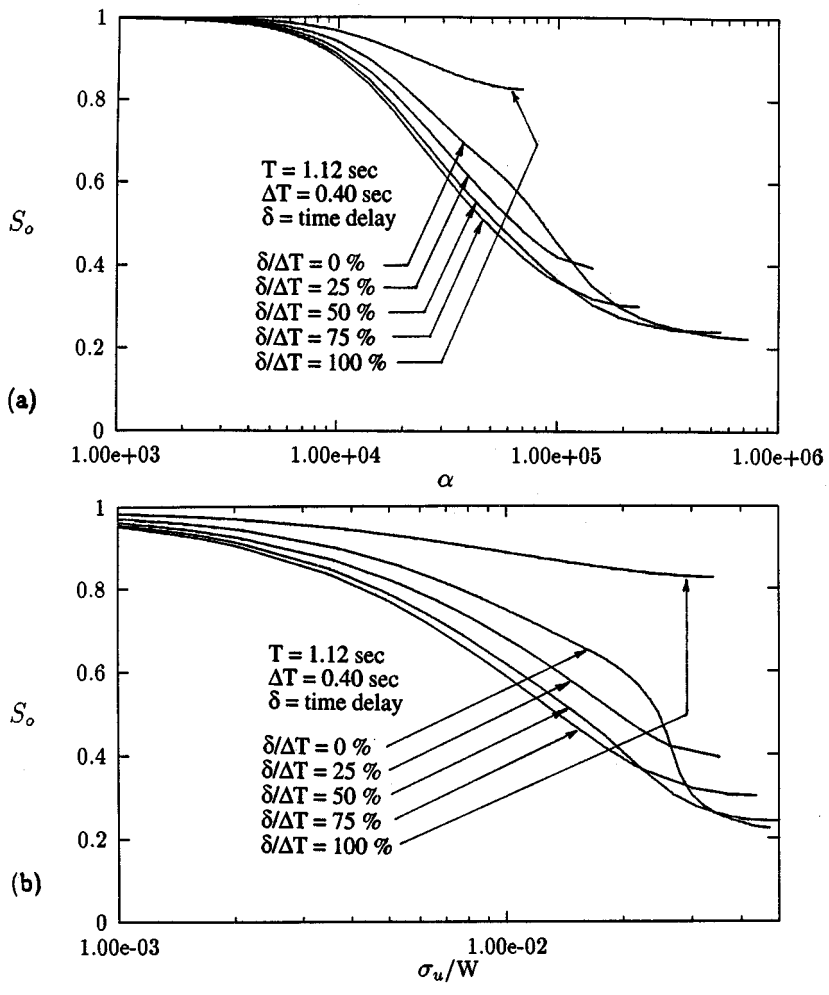

Figure 12. The effects of time delay on controller performance for the five storey shear beam model, with a specific sampling interval: (a) trends in S_0 as a function of the scalar weight α; and (b) trade-off curves exhibiting the control performance as a function of the control energy required

no delay. Thus for the cases considered, sampled data controllers were able to 'tolerate' small time delays for both the seismic engineering applications of this study.

The effects of time delay are marked for the planar frame, as seen from Figure 14. In this case, only when $\delta/\Delta T \leqslant 25$ per cent is the controller performance reasonable. The best controlled response corresponds to $S_0 \approx 0{\cdot}75$ with no time delays; with a time delay ratio $\delta/\Delta T = 25$ per cent, the best response is $S_0 \approx 0{\cdot}83$, and when δ is of the order of ΔT the actively controlled response is barely better than the passively controlled one ($S_0 \approx 0{\cdot}95$ or more).

For the results presented so far, the only seismic excitation considered was the NS component of the 1940 El Centro earthquake. To further analyze the control performance for other seismic

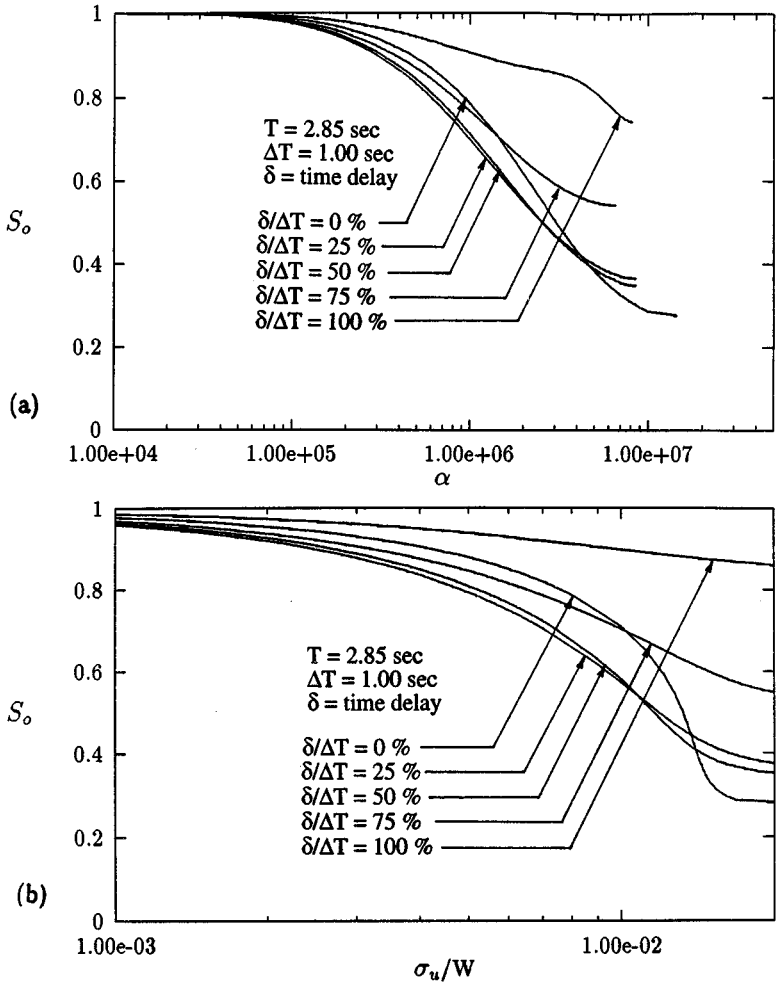

Figure 13. The effects of time delay on controller performance for the eight storey shear beam model, with a specific sampling interval: (a) trends in S_0 as a function of the scalar weight α; and (b) trade-off curves exhibiting the control performance as a function of the control energy required

excitations, five other earthquake records were considered. These were the 1949 Puget Sound earthquake, the 1971 San Fernando Valley earthquake, the 1994 Northridge earthquake, filtered white noise, and Gaussian white noise. Controlled responses of the Five and Eight Storey Shear Beam Examples during these earthquakes were simulated, and the results are summarized in Tables I and II along with those for the 1940 El Centro earthquake.

The tables show that the designs are quite effective in reducing the roof displacements for all the seismic excitations considered. Similarly, the RMS roof accelerations are also uniformly reduced. For the cases considered, the peak accelerations are either largely unaffected (San Fernando and Northridge earthquakes), uniformly reduced (1940 El Centro, filtered while noise and Gaussian

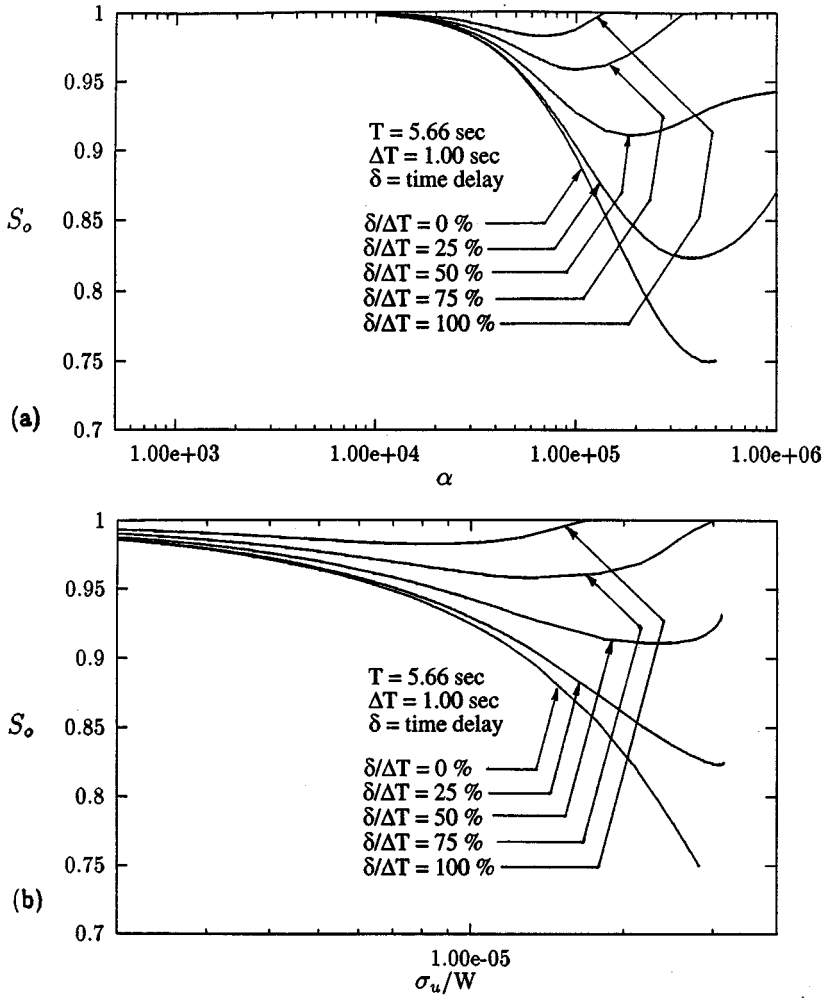

Figure 14. The effects of time delay on controller performance for the planar frame, with a specific sampling interval: (a) trends in S_0 as a function of the scalar weight α; and (b) trade-off curves exhibiting the control performance as a function of the control energy required

white noise earthquakes), or show a slight increase of upto 3–4 per cent (Puget Sound, WA earthquake). In all these cases the peak control force never exceeds 2–3 per cent of the building weight, and the RMS force is less than 1 per cent of the building weight.

Similarly Table III summarizes the trends in RMS/peak roof responses and control force for the Planar Frame subjected to wind excitation, for different values of the weight α. It is noted that both the RMS and peak displacements and accelerations are uniformly reduced. Also, for the assumed parameters, the peak control force never exceeds 0·00006 per cent of the building weight, and the RMS force never exceeds 0·00003 per cent of the building weight.

Table I. Summary of controlled responses of the Five Storey Shear Beam Example with an active base isolator for different earthquake excitations, with $\Delta T/T = 0{\cdot}25$

Example earthquake record	Gain parameter α ($\times 10^6$)	Roof displ. ratios*		Roof accel. ratios*		Control force/weight	
		Peak P_0 (%)	Std. Devn. S_0 (%)	Peak $\tilde{P}_0$ (%)	Std. Devn. $\tilde{S}_0$ (%)	Peak u_0/W (%)	Std. Devn. σ_u/W (%)
El Centro (1940) NS Component	1	96·24	82·79	96·35	83·47	0·60	0·27
	2	88·45	62·47	89·04	64·13	1·80	0·65
	3	80·15	52·90	81·76	55·12	2·93	1·00
Puget Sound, WA (1949)	1	86·73	84·14	89·55	86·18	0·64	0·20
	2	67·64	61·89	74·49	67·07	1·51	0·49
	3	57·20	49·85	66·81	57·01	2·33	0·71
San Fernando Valley (1971)	1	99·25	85·33	100·01	88·58	0·12	0·04
	2	98·13	70·66	100·04	77·54	0·39	0·12
	3	96·63	63·33	100·06	72·17	0·71	0·19
Northridge (1994) Sylmar Obs.	1	89·57	86·23	100·10	96·51	0·14	0·04
	2	76·52	64·49	100·19	91·69	0·39	0·10
	3	65·22	49·28	100·08	89·07	0·64	0·14
Filtered White noise ($\omega_g = \pi$, $\zeta_g = 0{\cdot}3$)	1	86·03	87·07	83·89	85·56	0·17	0·08
	2	69·10	68·83	65·56	64·83	0·47	0·19
	3	58·48	57·43	58·38	51·18	0·68	0·29
Gaussian White noise $\mathscr{E}\{w\} = 0$, $\mathscr{E}\{w^2\} = 1$	1	90·43	82·21	93·94	89·99	0·26	0·11
	2	73·01	60·65	84·13	79·21	0·67	0·25
	3	63·93	50·94	78·17	74·86	1·13	0·39

*Active base isolation/passive base isolation

The preceding discussions suggest that sampled data controllers may have good potential for use in structural control. It also appears that such controllers can tolerate small time delays without sacrificing control performance severely. The extent of time delay which could be tolerated appears larger for the seismic engineering examples studied here. In recent times the implementation of (such) digital controllers has become easier due to the widespread use of computers and advances in software. In view of this, sampled data control appears to be a cost-effective solution for vibration control problems. However, several design aspects need to be studied in further depth, namely the effect of actuator dynamics, actuator saturation, unmodelled dynamics, the ability of actuators to track the control signal, development of software to implement sampled data control, etc. Some of these issues have already received attention in recent times, and integration of the present approach with techniques developed by other researchers, along with in-depth studies and analyses of the design aspects involved may be topics for further research in this area.

Table II. Summary of controlled responses of the Eight Storey Shear Beam Example with an active base isolator for different earthquake excitations, with $\Delta T/T = 0{\cdot}25$

Example earthquake record	Gain parameter α ($\times 10^6$)	Roof displ. ratios*		Roof accel. ratios*		Control force/weight	
		Peak P_0 (%)	Std. Devn. S_0 (%)	Peak $\tilde{P}_0$ (%)	Std. Devn. $\tilde{S}_0$ (%)	Peak u_0/W (%)	Std. Devn. σ_u/W (%)
El Centro (1940) NS Component	1	65·10	53.62	91·31	70·55	1·60	0·77
	2	45·79	36·52	81·52	63·12	2·22	1·00
	3	41·68	28·66	74·72	60·32	2·85	1·09
Puget Sound, WA (1949)	1	67·51	68·71	101·8	94·11	0·90	0·28
	2	62·80	55·65	103·7	91·98	1·71	0·42
	3	63·28	51·78	104·4	91·48	2·43	0·54
San Fernando Valley (1971)	1	75·00	62·58	100·00	93·28	0·18	0·08
	2	81·35	56.11	100·00	92·70	0·39	0·13
	3	84·60	52·52	100·00	92·93	0·59	0·17
Northridge (1994) Sylmar Obs.	1	92·02	86·06	100·00	99·80	0·19	0·06
	2	89·36	80·61	100·00	99·78	0·36	0·12
	3	92·90	64·85	100·00	99·78	0·52	0·15
Filtered White noise ($\omega_g = \pi$, $\zeta_g = 0{\cdot}3$)	1	78·16	72·01	99·16	74·44	0·94	0·36
	2	71·24	64·42	95·67	67·96	1·71	0·62
	3	59·07	58·64	87·43	68·15	2·11	0·80
Gaussian White noise $\mathscr{E}\{w\} = 0$, $\mathscr{E}\{w^2\} = 1$	1	62·35	59·39	82·81	87·18	1·16	0·40
	2	48·66	43·86	78·36	83·99	1·65	0·56
	3	43·25	37·55	77·72	83·11	1·99	0·66

*Active base isolation/passive base isolation

Table III. Summary of controlled responses of the Planar Frame Example with an active mass damper subjected to simulated wind gust excitation, with $\Delta T/T = 0{\cdot}25$

Gain parameter α ($\times 10^6$)	Roof displ. ratios*		Roof accel. ratios*		Control force/weight	
	Peak P_0 (%)	Std. Devn. S_0 (%)	Peak $\tilde{P}_0$ (%)	Std. Devn. $\tilde{S}_0$ (%)	Peak u_0/W (%)	Std. Devn. σ_u/W (%)
0·5	70·66	79·08	74·85	80·23	4·80	2·40
1·0	74·81	78·59	78·12	79·45	5·00	2·41
1·5	75·52	78·59	78·64	79·37	5·60	2·42
2·0	74·66	78·58	78·01	79·46	5·61	2·42

*Active mass damper control/passive mass damper

4. CONCLUDING REMARKS

In this study, an optimal control method using sampled data proposed by Khargonekar *et al.*[5] was considered for structural control applications. Using a constant sampling interval and zero-order sample/hold devices, the optimal control signal was generated based on incomplete data. Numerical examples of two buildings with active base isolators and a 163-m planar frame with an active mass damper were considered. The 1940 El Centro earthquake, the 1949 Puget Sound earthquake, the 1971 San Fernando Valley earthquake, the 1994 Northridge earthquake and filtered/unfiltered white Gaussian noise were used as excitations for the actively base isolated building examples. For the planar frame, sinusoidal gusts with a frequency close to the period of the frame were used.

For the examples studied here, it was found that such controllers have good potential for use in vibration control. Also, for the examples studied and the parameters assumed, it was found that the controllers were able to tolerate small time delays without sacrificing performance severely.

Due to the widespread use of digital computers and the increasing trends in software development, implementation of digital controllers has become easier. These controllers are also easier to maintain than their analog counterparts in the long run. In view of this, sampled data control appears to be a cost-effective solution for vibration problems. However, there are many issues which remain to be explored, for instance, tracking capability of actuators, effects of actuator dynamics, saturation, incorporation of sampled-data technology into structural monitoring systems, etc. These areas may be investigated in future studies.

ACKNOWLEDGEMENTS

This study was sponsored by the National Science Foundation through grant 9496273-CMS. Dr Elenora Sabadell is the Program Director. Her guidance and advice are appreciated.

REFERENCES

1. J. Rodellar, L. L. Chung, T. T. Soong and A. M. Reinhorn, 'Experimental digital control of structures', *J. Engng. Mech. ASCE* **115**, 1245–1261 (1989).
2. W. Cui, K. Nonami and H. Nishimura, 'Experimental study on active vibration control of structures by means of h-infinity control and H-2 control', *JSME Int. J. Ser. C* **37**, 462–467 (1994).
3. S. J. Shelley, K. L. Lee, T. Aksel and A. E. Aktan, 'Active-control and forced vibration studies on highway bridge', *J. Struct. Engng. ASCE* **121**, 1306–1312 (1995).
4. J. Ackermann, *Sampled-data Control Systems*: *Analysis and Synthesis*, *Robust System Design*, Springer, Berlin, 1985.
5. P. P. Khargonekar and N. Sivashankar, 'H-2 optimal control for sampled-data systems', *System Control Lett.* **17**, 425–436 (1991).
6. J. M. Kelly, G. Leitmann and A. G. Soldatos, 'Robust control of base-isolated structures under earthquake excitation', *J. Optim. Theory Appl.* **53**(2), 159–180 (1987).
7. T. Y. Yang, D. G. Liaw, D. S. Hsu and H. C. Fu, 'Simple model for optimal control of tall buildings', *J. Struct. Engng. ASCE* **119**, 902–919 (1993).
8. W. E. Saul, P. Jayachandran and A. H. Peyrot, 'Response to stochastic wind of *N*-degree tall buildings', *J. Struct. Div. ASCE* **102**, 1059–1075 (1976).
9. A. Kareem, 'Mitigation of wind induced motion of tall buildings', *J. Wind Engng. Ind. Aerodyn.* **11**, 273–284 (1983).
10. H. Liu, *Wind Engineering*: *A Handbook For Structural Engineers.* Prentice-Hall, Englewood Cliffs, NJ, 1991.

